UBE2K regulated by IGF2BP3 promotes cell proliferation and stemness in pancreatic ductal adenocarcinoma

WEN FU[1,2], XIANGXIANG LEI[2,3], QILIANG LU[1,2], JI ZHANG[4,2], JINHUI GUO[1,2], JIE ZHAO[4,2], XIANGMIN TONG[1,2] and XIAOGE HU[2,5]

[1]Qingdao Medical College, Qingdao University, Qingdao, Shandong 266071; [2]The Key Laboratory of Tumor Molecular Diagnosis and Individualized Medicine of Zhejiang Province, Zhejiang Provincial People's Hospital, Affiliated People's Hospital, Hangzhou Medical College, Hangzhou, Zhejiang 310014; [3]Institute of Basic Medicine and Forensic Medicine, Hangzhou Medical College, Hangzhou, Zhejiang 310053; [4]Zhejiang University of Technology; [5]Department of Hepatobiliary and Pancreatic Surgery, Zhejiang Provincial People's Hospital, Affiliated People's Hospital, Hangzhou Medical College, Hangzhou, Zhejiang 310014, P.R. China

Received October 26, 2022; Accepted February 16, 2023

DOI: 10.3892/ijo.2023.5500

Abstract. Pancreatic ductal adenocarcinoma (PDAC) is a noteworthy malignant carcinoma with an unsatisfactory prognosis attributed to late diagnosis. Ubiquitin-conjugating enzyme E2K (UBE2K) has been found to serve important roles in a number of diseases. However, its function and the exact molecular mechanism of UBE2K in PDAC remain to be elucidated. The present study discovered that UBE2K was expressed at high levels and indicated the poor prognosis of patients with PDAC. Following this, the CCK-8, colony formation, and sphere formation assays showed that UBE2K promoted proliferation and the stemness phenotype of PDAC cells *in vitro*. Evidence from subcutaneous tumor-bearing nude mice experiments further confirmed that UBE2K enhanced PDAC cell tumorigenesis *in vivo*. Additionally, the present study demonstrated that insulin-like growth factor 2 RNA binding protein 3 (IGF2BP3) functioned as an RNA-binding protein to increase UBE2K expression by enhancing the RNA stability of UBE2K. The knockdown or overexpression of IGF2BP3 could attenuate the change in cells growth induced by the overexpression or knockdown of UBE2K. In summary, the findings indicated the oncogenic roles of UBE2K in PDAC. In addition, IGF2BP3 and UBE2K constitute a functional axis to regulate the malignant progression of PDAC.

Correspondence to: Professor Xiaoge Hu or Professor Xiangmin Tong, The Key Laboratory of Tumor Molecular Diagnosis and Individualized Medicine of Zhejiang Province, Zhejiang Provincial People's Hospital, Affiliated People's Hospital, Hangzhou Medical College, 158 Shangtang Road, Gongshu, Hangzhou, Zhejiang 310014, P.R. China
E-mail: huxiaoge2008xmu@163.com
E-mail: tongxiangmin@163.com

Key words: ubiquitin-conjugating enzyme E2K, insulin-like growth factor 2 RNA binding protein 3, proliferation, stemness, pancreatic ductal adenocarcinoma

Introduction

Currently, pancreatic ductal adenocarcinoma (PDAC) is the seventh commonest cause of deaths in the world (1). Due to delayed diagnosis and a lack of effective therapeutic regimens, the 5-year survival rate in PDAC is ~6% (2). Surgical resection may be a potential therapeutic method for patients with early-stage disease, but it is insufficient in advanced-stage disease (3). The poor prognosis highlights the need to identify more molecular markers to improve early diagnosis and reduce mortality. Thus, more in-depth research is necessary to determine the mechanisms underlying the pathogenesis of PDAC.

Ubiquitylation is an important post-translational modification that helps maintain protein homeostasis in eukaryotic cells via the marking of proteins by ubiquitin, which are subsequently eliminated by the proteasome (4-7). E2 enzymes, which are core constituents of the ubiquitin system, can influence the signal generation in ubiquitylation and alter the eventual consequences of substrate proteins (8). Ubiquitin-conjugating enzyme E2K (UBE2K) is a type of class II E2 group enzyme, also referred to as E2-25K or HIP-2, which can contribute to the combination of K48-linked ubiquitin chains (9,10). UBE2K serves a number of roles in various diseases. For instance, UBE2K serves important roles in nervous system diseases, including Huntington's disease (HD), Alzheimer's disease (AD), Parkinson's disease (PD), and amyotrophic lateral sclerosis (ALS) (11-14). Findings from previous studies have also demonstrated that UBE2K serves vital roles in tumors and can be a target in cancer therapy (15,16). For example, ixazomib exhibits antitumor potential by targeting UBE2K in myeloma cells (15) and the overexpression of UBE2K promotes gastric cancer progression *in vitro* and *in vivo* (16). However, its functions in PDAC remain to be elucidated.

RNA-binding proteins (RBPs) can regulate the fate of RNA by modulating their stabilization and degradation to influence gene expression in cancer cells (17). Insulin-like growth factor 2 RNA binding protein 3 (IGF2BP3) belongs to the insulin like growth factor 2 RNA binding protein family (18), which broadly participates in the progression of multiple tumors. In recent studies, IGF2BP3 was shown to promote malignant tumors progression by encouraging the stabilization of downstream targets. For example, it enhanced the stability of RCC2 expression in myeloid leukemia, cooperated with LINC00958 to maintain the expression of E2F3 in endometrial carcinoma, interacted with METTL3 to influence the expression of PD-L1 to promote immune escape in breast carcinoma, and sustained the expression of SIX4 in ovarian tumor cells (19-22). However, whether IGF2BP3 regulates UBE2K expression in PDAC has yet to be reported.

The present study found that UBE2K expression was higher in PDAC cell lines and tissues compared with that in normal cell lines and tissues. It further showed that UBE2K overexpression encouraged cell proliferation and stemness-like phenotype, while UBE2K knockdown inhibited the proliferation and stemness-like phenotype. In addition, IGF2BP3 was found to be an RNA-binding protein that enhanced UBE2K RNA stability, thus promoting UBE2K expression. Finally, IGF2BP3 and UBE2K were demonstrated to form a functional axis through functional rescue experiments. Collectively, the results revealed the oncogenic roles of the IGF2BP3/UBE2K axis in the malignant progression of PDAC, which might provide novel insights into targeted therapy for PDAC.

Materials and methods

Databases. The gene expression profiling interactive analysis (GEPIA) database (http://gepia.cancer-pku.cn/) can analyze the RNA sequencing data of tumors and normal samples from The Cancer Genome Atlas (TCGA) and the GTEx projects by clicking to obtain gene expression profile, correlation analysis and patient survival probability (23). The present study detected the expression levels of UBE2K between 179 PAAD tumor tissues and 171 corresponding normal tissues. In addition, the overall survival rate (OS) and the correlation between IGF2BP3 and UBE2K in PAAD were also analyzed in GEPIA.

The Kaplan Meier plotter (https://kmplot.com) is a web tool to assess the survival probability in tumor samples including PDAC from the GEO and TCGA databases. The present study searched the OS and relapse free survival rate (RFS) between higher and lower UBE2K RNA expression levels in PDAC patients.

Cells culture. AsPC-1, BxPC-3, PANC-1, SW1990, and HPNE cells were maintained in the Key Laboratory of Tumor Molecular Diagnosis and Individualized Medicine of Zhejiang Province. PANC-1, HPNE, and SW1990 cells were cultured in DMEM (Biological Industries). Meanwhile, AsPC-1 and BxPC-3 cells were cultured in 1640 medium (Biological Industries). The cells were all cultured in media supplemented with 10% fetal bovine serum (Biological Industries) supplemented with 1% penicillin/streptomycin in an incubator with 5% CO_2 at 37˚C condition.

Cells transduction and transfection. Lentivirus for UBE2K overexpression or knockdown was purchased from Genomeditech Biotechnology (Shanghai) Co., Ltd. 293T cells were used as the interim cell line to generate the packaged lentivirus. The concentration of short hairpin (sh)NC (5'-TTCTCCGAACGTGTCACGT-3'), shUBE2K#1 (5'-TGACTCTCCGCACGGTATTAT-3'), and shUBE2K#2 (5'-GCGAATCAAGCGGGAGTTCAA-3') was $1x10^8$ TU/ml, $1.06x10^8$ and $2.11x10^8$ TU/ml, respectively. BxPC-3 and PANC-1 cells were infected by virus with an MOI of 20 in a biological safety cabinet at room temperature. Polybrene (6 μg/ml) was used to improve transfect efficiency. After 72 h, stably transduced cells were selected by treatment with blasticidin S (30 μg/ml) at 37˚C for 2 weeks. Scramble short interfering (si)RNA and siRNAs targeting IGF2BP3 were purchased from Shanghai GenePharma Co., Ltd. The sequences of the siRNAs were: siNC (sense: 5'-UUCUCCGAACGUGUCACGUTT-3', antisense: 5'-ACGUGACACGUUCGGAGAATT-3'), siIGF2BP3#1 (sense: 5'-GGCAAAGGAUUCGGAAACUTT-3', antisense: 5'-AGUUUCCGAAUCCUUUGCCTT-3') and siIGF2BP3#2 (sense: 5'-GGCUCAGGGAAGAAUUUAUTT-3', antisense: 5'-AUAAAUUCUUCCCUGAGCCTT-3'). The IGF2BP3 and PCDNA3.1 plasmids were maintained in the Key Laboratory of Tumor Molecular Diagnosis and Individualized Medicine of Zhejiang Province. Cells were transfected with 10 μl (20 μM) siRNA or 2 μg plasmid using the Lipofectamine® 3000 (Invitrogen; Thermo Fisher Scientific, Inc.) based on the manufacturer's instructions in a biological safety cabin at room temperature for 10-15 min. Subsequent experiments were performed after the cells had been incubated at 37˚C for 48 h.

Reverse transcription-quantitative (RT-q) PCR. Entire RNAs were extracted from cells (~90% confluency)and tissues using an RNA quick purification kit (ES science; cat. no. RN001) according to the manufacturer's instructions. Nano-Drop One (Thermo Fisher Scientific, Inc.) was used to confirm the concentration and quality of RNAs, for which the ratio of absorption at 260-280 nm was between 1.9-2.2. Following this, complementary DNA (cDNA) was synthesized using s1000 (Bio-Rad Laboratories, Inc.) with a prime script RT reagent kit (Takara Bio, Inc.; cat. no. RR037A-1) according to the manufacturer's protocol. RT-qPCR was conducted using SYBR Green (Shanghai Yeasen Biotechnology Co., Ltd.; cat. no. 11184ES08) according to the manufacturer's protocol by 7500 real-time PCR system under the following conditions: Holding stage at 95˚C for 2 min, cycling stage 40 cycles at 95˚C for 10 sec, and 60˚C for 30 sec, the melt curve stage at 95˚C for 15 sec, 60˚C for 30 sec and 95˚C for 5 sec. Each experiment was repeated three times. For the calculation of relative RNA expression, the IGF2BP3 and UBE2K expression levels were normalized to GAPDH expression using $2^{-\Delta\Delta Cq}$ method (24). The sequences of primer used were as follows: UBE2K forward 5'-CGCGGTGCAGCGAATC-3' and reverse 5'-TTGCTCGTCTCCTCGCTCTT-3'. IGF2BP3 forward 5'-CCATGTGATTTGCCTCTGCG-3' and reverse 5'-ACTGGGTCTGTTTGGTGATGT-3' and GAPDH forward 5'-GTCTCCTCTGACTTCAACAGCG-3' and reverse 5'-ACCACCCTGTTGCTGTAGCCAA-3'.

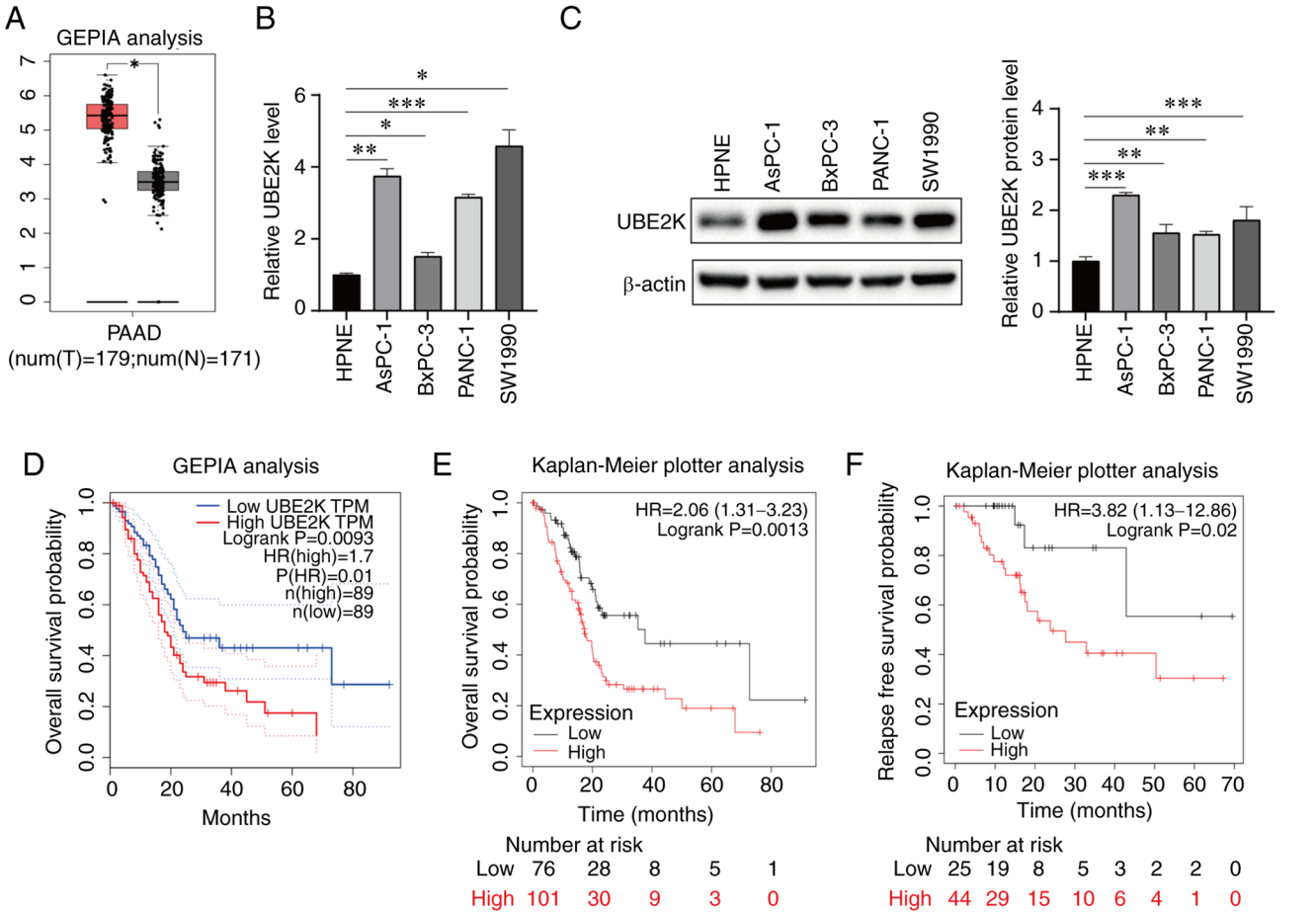

Figure 1. UBE2K is upregulated in tissues and cell lines of PDAC and predicts a poor prognosis. (A) UBE2K was highly expressed in PDAC tissues (left, red) compared with normal tissues (right, black) in GEPIA. (B) Reverse transcription-quantitative PCR and (C) western blotting results indicated that UBE2K was highly expressed in PDAC cell lines (AsPC-1, BxPC-3, PANC-1 and SW1990) compared with HPNE in RNA and protein levels. The databases of (D) GEPIA and (E) Kaplan-Meier plotter indicated higher UBE2K expression correlated to lower overall survival in PDAC patients. (F) Kaplan-Meier plotter survival analysis indicated that patients with higher expression of UBE2K exhibited lower relapse free survival rate. *P<0.05, **P<0.01, ***P<0.001. UBE2K, ubiquitin-conjugating enzyme E2K; PDAC, pancreatic ductal adenocarcinoma; GEPIA, gene expression profiling interactive analysis; HPNE, normal human pancreatic cells; HR, hazard ratio.

Western blotting. Entire protein content of cells and tissues was extracted using lysis buffer (Beyotime Institute of Biotechnology; cat. no. P0013) plus phenylmethylsulfonyl fluoride solution (Beyotime Institute of Biotechnology; cat. no. ST507-10 ml) and protease inhibitor cocktail (bimake; cat. no. B14002) which were protease inhibitors. The protein concentration was determined using the Pierce BCA protein assay kit (Thermo Fisher Scientific, Inc.; cat. no. 23225). After boiling for 10 min at 95˚C, equal quantities of protein (20-40 μg) were separated by 8-10% SDS-PAGE and transferred to PVDF membranes (MilliporeSigma; cat. no. IPVH00010). Then the 0.45 μm membrane was blocked in 5% skimmed milk for 1 h at room temperature. After washing, the membrane was cut into pieces using a page-ruler pre-stained protein ladder (Thermo Fisher Scientific, Inc.; cat. no. 26617) and based on the molecular weight of the proteins. The pieces of the membrane were treated overnight with primary antibodies, including anti-UBE2K (Proteintech Group, Inc.; cat. no. 11834-3-AP, 1:2,000. CST Biological Reagents Co., Ltd.; cat. no. 8226; 1:1,000), anti-IGF2BP3 (Proteintech Group, Inc.; cat. no. 14642-1-AP; 1:3,000), anti-NANOG (CST Biological Reagents Co., Ltd.; cat. no. 4903; 1:2,000), anti-LIN28B (CST Biological Reagents Co., Ltd.; cat. no. 4196; 1:1,000), GAPDH (Affinity Biosciences; cat. no. AF7021; 1:6,000), and anti-β-ACTIN (Affinity Biosciences; cat. no. AF7018; 1:5,000) at 4˚C. Then, the pieces were washed three times with TBST (containing 0.1% Tween-20), and treated with the goat anti-rabbit IgG secondary antibody (Thermo Fisher Scientific, Inc.; cat. no. 31460, 1:20,000) for 1 h at room temperature. This was followed by repeated washing with TBST three times, and the pieces were incubated in Clarity™ Western ECL Substrate (Bio-Rad Laboratories, Inc.) away from light several minutes for further visualization. Finally, the protein content was analyzed by ImageJ software (version 1.52v; National Institutes of Health).

Cell Counting Kit-8 assay. To measure the cell proliferation ability, 5x10^3 cells were seeded in a 96-well plate. After 24, 48, and 72 h, 100 μl complete medium and 10 μl of the CCK-8 assay reagent (Shanghai Yeasen Biotechnology Co., Ltd.; cat. no. 40203ES80) were added to each well. The cells were incubated for >1 h, and the absorbance at 450 nm was measured.

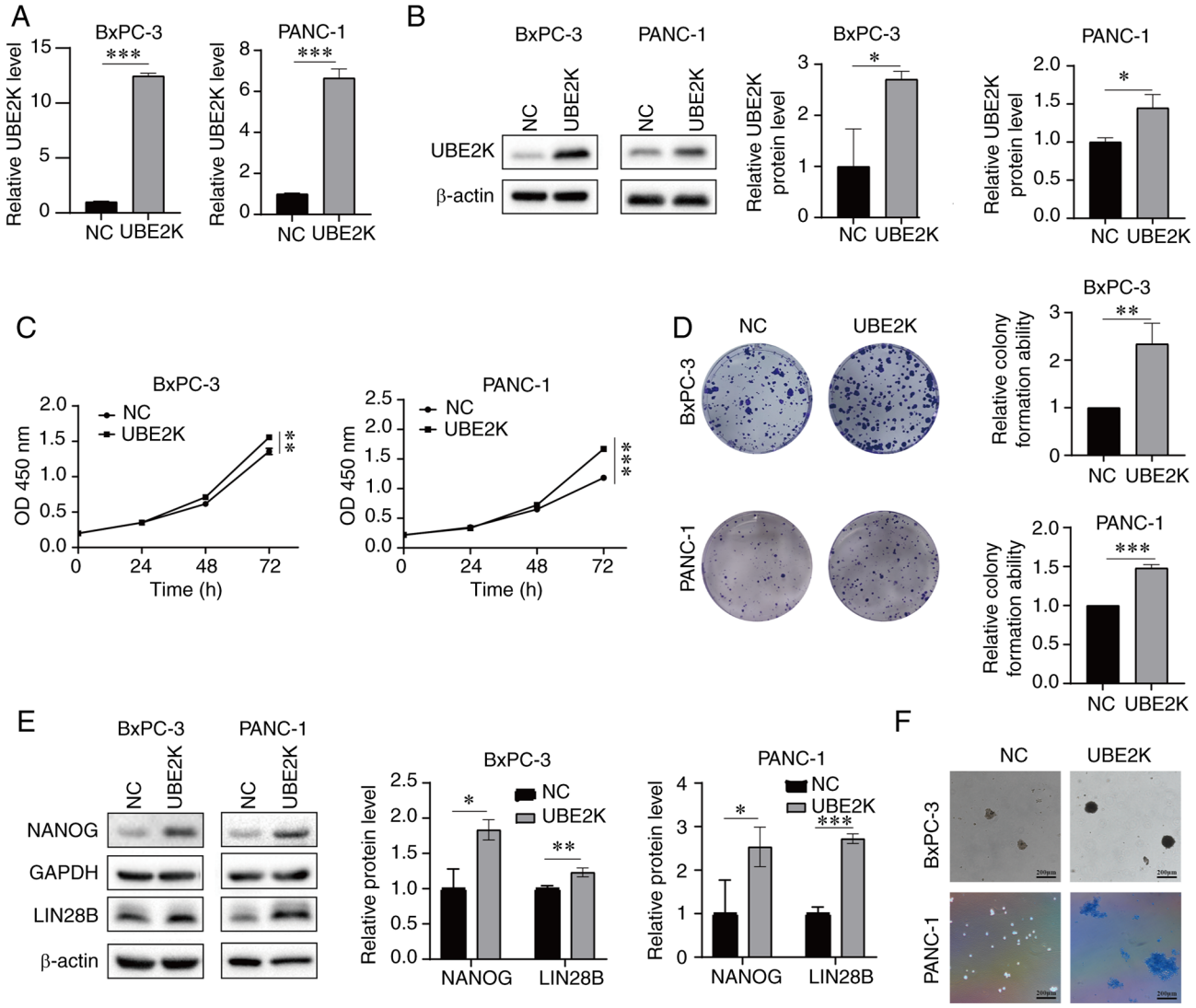

Figure 2. Overexpression of UBE2K promotes proliferation and stemness of PDAC *in vitro*. (A) Reverse transcription-quantitative PCR and (B) western blotting results confirmed that overexpression stably transduced strains of UBE2K was established in BxPC-3 and PANC-1. (C) CCK-8 and (D) colony formation assays indicated overexpression of UBE2K promoted proliferation ability. (E) Western blotting results indicated overexpression of UBE2K promoted stemness genes expression. (F) Sphere formation results indicated the overexpression of UBE2K increased the size of sphere (scale bar, 200 μm). *P<0.05, **P<0.01, ***P<0.001. UBE2K, ubiquitin-conjugating enzyme E2K; PDAC, pancreatic ductal adenocarcinoma; NC, negative control.

Colony formation assay. To detect the colony-forming ability of the cells, 750 cells were seeded in 6-well plates. Then, the plates were maintained in complete medium for 12 days. When the colonies were formed, the cells were fixed with polyformaldehyde for 30 min at room temperature and then stained with 0.5% of crystal violet for 1 h at room temperature. Finally, colonies (>50 cells) visible on the surface were manually counted.

Sphere formation assay. To measure the cell stemness, 5x10^4 cells were seeded in ultralow attachment six-well plates. The cells were cultured in DME/F-12 (1:1) medium (Biological Industries) containing epidermal growth factor (10 ng/ml), basic fibroblast growth factor (10 ng/ml) and N2. Following this, the spheres were cultured for 14 days and then imaged by inverted fluorescence microscope (Nikon) for further analysis.

RNA stability assay. BxPC-3 cells were transfected with siRNAs (siNC, siIGF2BP3#1 and siIGF2BP3#2) in 6-well plates using Lipofectamine® 3000 transfection reagent (Thermo Fisher Scientific, Inc.) as above. After 48 h, actinomycin D was used to treat the cells for 0, 6, 12, and 18 h at 37˚C. Total RNA was isolated and subjected to RT-qPCR to analyze gene expression as above. GAPDH was used as an endogenous control.

Subcutaneous xenografts in nude mice. A total of 23 4-week old female BALB/C athymic nude mice (17-21 g) were acquired from the Shanghai SLAC laboratory Animal Co., Ltd. The mice were maintained in SPF conditions which included 22˚C room temperature, 55% humidity and 12-h light/dark cycle and had free access to food and water. UBE2K stable-expression BxPC-3 cells (UBE2K) and the corresponding control cells (NC) were harvested and resuspended in serum-free 1640 medium (4x10^6 cells/150 μl). UBE2K stable-knockdown BXPC3 cells (shUBE2K#1, shUBE2K#2) and their corresponding control cells (shNC) were also harvested and resuspended in serum-free 1640 medium (4x10^6 cells/150 μl). Then, 150 μl of the cell suspension was subcutaneously injected into the

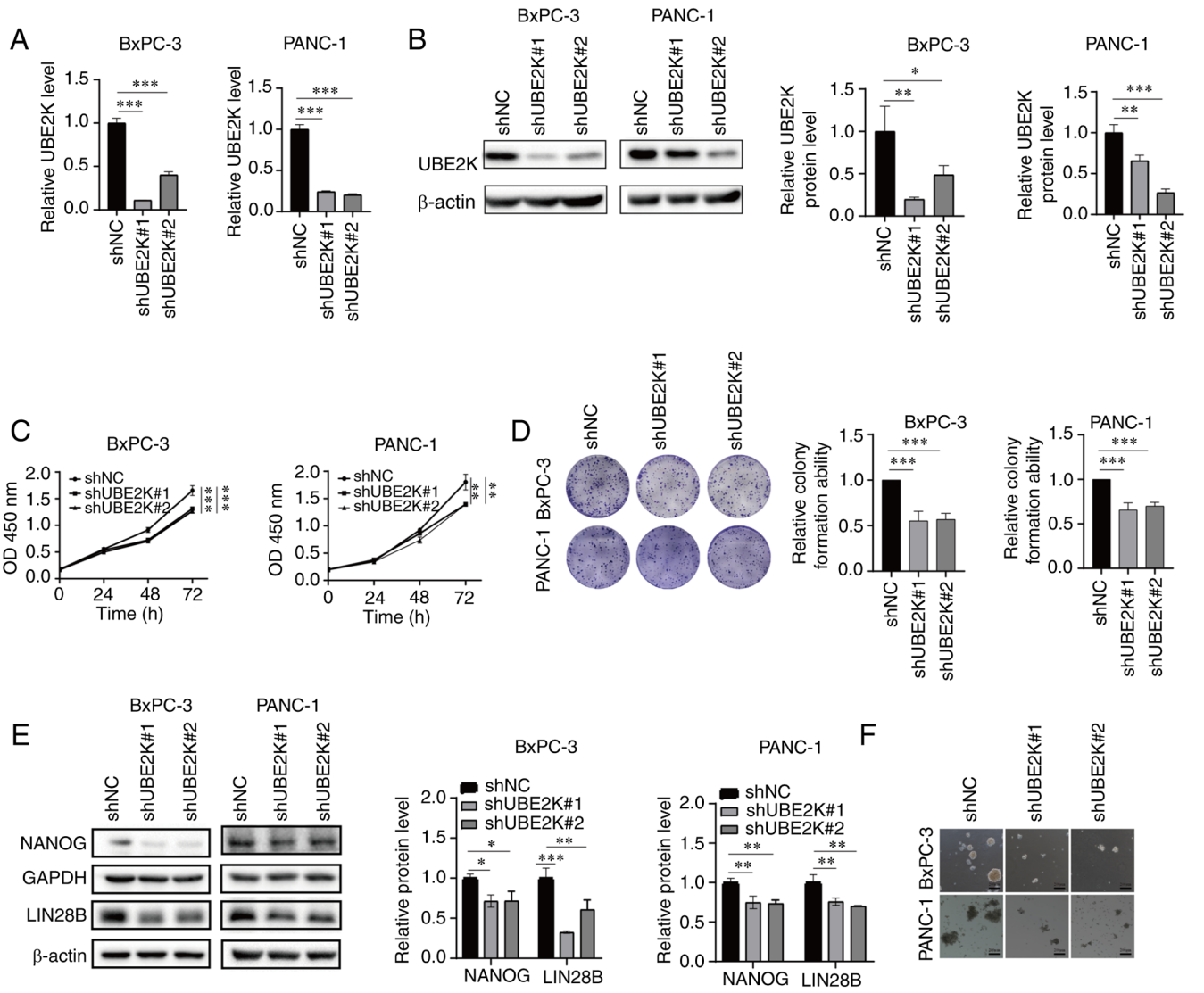

Figure 3. Knockdown of UBE2K suppresses proliferation and stemness of PDAC *in vitro*. (A) Reverse transcription-quantitative PCR and (B) western blotting results confirmed that knockdown stably transduced strains of UBE2K was established in BxPC-3 and PANC-1. (C) CCK-8 and (D) colony formation assays indicated knockdown of UBE2K reduced proliferation ability. (E) Western blotting results indicated knockdown of UBE2K decreased stemness genes expression. (F) Sphere formation results indicated the knockdown of UBE2K decreased the size of spheres (scale bar, 200 μm). *P<0.05, **P<0.01, ***P<0.001. UBE2K, ubiquitin-conjugating enzyme E2K; PDAC, pancreatic ductal adenocarcinoma; NC, negative control; sh, short hairpin.

right flank of each nude mouse. After injection, the tumor was measured every 5 days and the tumor volume was calculated as follows: tumor volume (mm^3)=(length x $width^2$)/2. At the appropriate time, the mice were sacrificed by CO_2 euthanasia with 60% per minute of container volume replacement. Then the tumors were harvested for western blotting and RT-qPCR analysis. The above experiments on nude mice were approved by the animal ethics committee at Zhejiang Provincial People's Hospital (approval no. A20220046).

Statistical analysis. Each experiment was repeated at least three times, and GraphPad Prism was used for statistical analysis. Continuous variables were presented in term of mean and standard error of mean (SEM). Differences between two groups were assessed using two-tailed t tests. Differences between multiple groups were assessed using one way ANOVA followed by Dunnett's test. P<0.05 was considered to indicate a statistically significant difference.

Results

UBE2K is expressed at high levels and indicates poor prognosis in PDAC. UBE2K was upregulated in PDAC compared with that in corresponding normal tissues, as analyzed from the data obtained from the GEPIA database (Fig. 1A). To comprehensively explore the expression of UBE2K in PDAC, the RNA and protein expression levels of UBE2K in PDAC cell lines (AsPC-1, BxPC-3, PANC-1, and SW1990) and human pancreatic ductal HPNE cells were detected. As shown in Fig. 1B and C, the RNA and protein levels of UBE2K were higher in PDAC cell lines compared with that in HPNE cells. Subsequently, the clinical prognosis of UBE2K expression in PDAC was analyzed using GEPIA and the Kaplan-Meier plotter database. Higher expression of UBE2K was associated with a shorter overall survival of patients with PDAC (Fig. 1D and E). Additionally, the Kaplan-Meier plotter database also showed that higher UBE2K expression was associated with a poorer RFS in PDAC

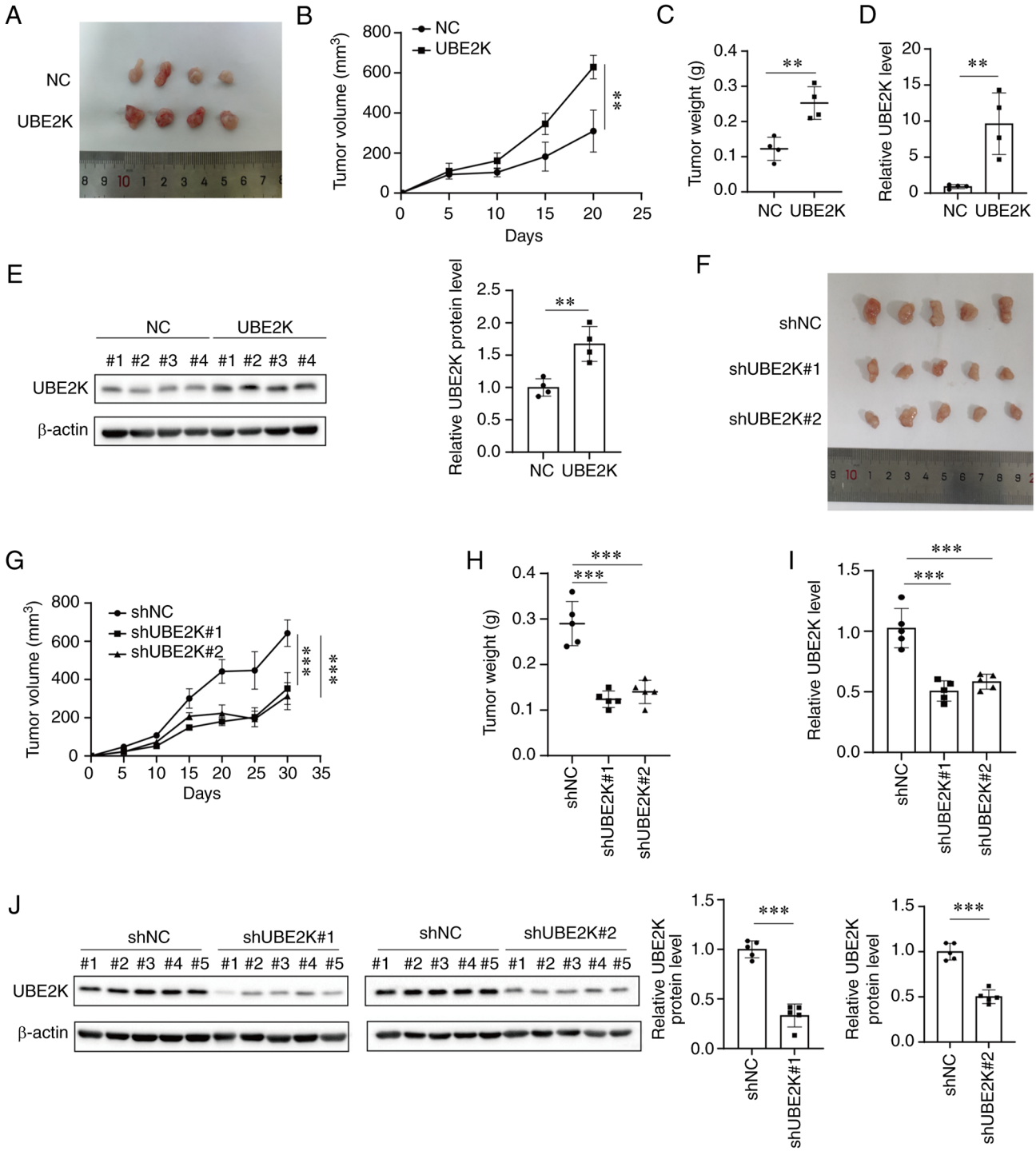

Figure 4. UBE2K promotes PDAC growth *in vivo*. (A) The tumors of UBE2K overexpression group were larger compared with NC in nude mice. The (B) volume and (C) weight of UBE2K overexpression group were larger compared with NC in the tumors of nude mice. The RNA (D) and (E) protein level of UBE2K overexpression group were higher compare to NC group. (F) The tumors of shNC group were larger compared with shUBE2K#1 and shUBE2K#2 groups in nude mice. The (G) volume and (H) weight of shNC groups were larger compared with shUBE2K#1 and shUBE2K#2 groups in the tumors of nude mice. The (I) RNA and (J) protein level of shNC were higher compared with shUBE2K#1 and shUBE2K#2 groups. **P<0.01, ***P<0.001. UBE2K, ubiquitin-conjugating enzyme E2K; PDAC, pancreatic ductal adenocarcinoma; NC, negative control; sh, short hairpin.

(Fig. 1F). Overall, UBE2K may be a potentially unfavorable biomarker for PDAC diagnosis.

UBE2K overexpression promotes cell proliferation and PDAC stemness. To explore the function of UBE2K in PDAC, stably UBE2K-overexpressing BxPC-3 and PANC-1 cells were generated using lentiviruses. RT-qPCR and western blotting were performed to verify the UBE2K overexpression rate in both RNA and protein levels (Fig. 2A and B). The CCK-8 and colony formation assays showed that UBE2K overexpression promoted PDAC cell growth *in vitro* (Fig. 2C and D). A significant upregulation of stemness-related protein expression was observed in UBE2K-overexpressing cells (Fig. 2E). In addition, UBE2K enhanced the sphere formation ability of PDAC cells, since

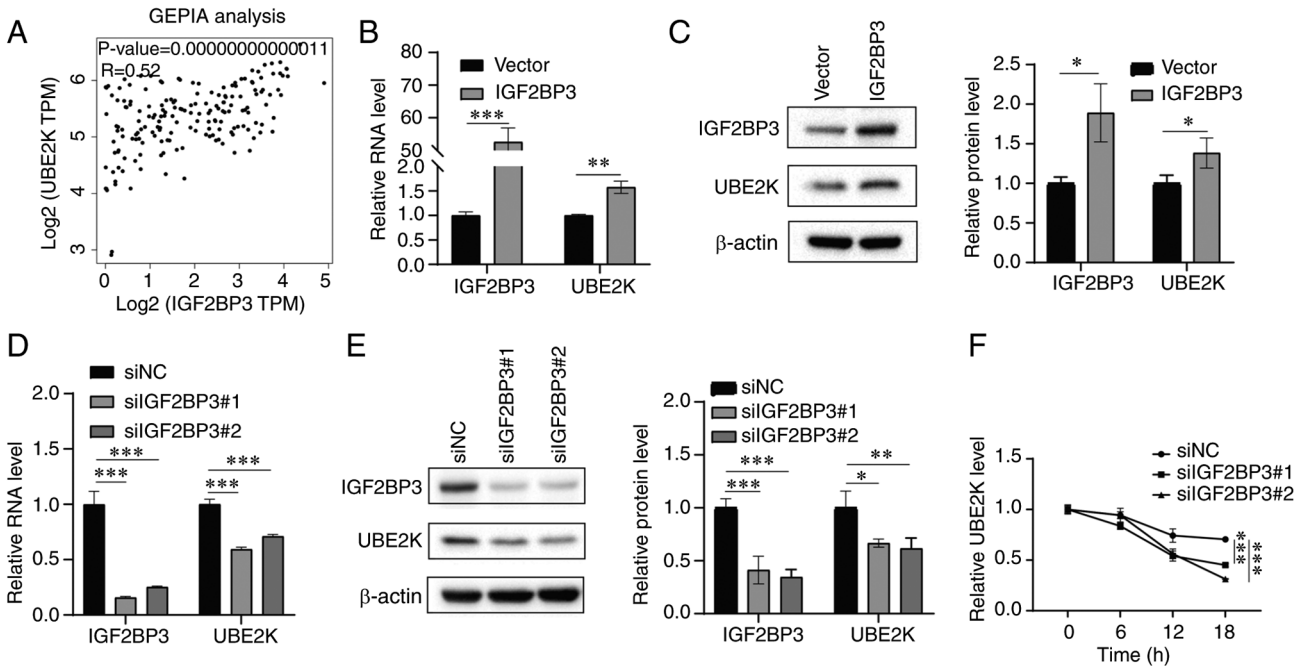

Figure 5. UBE2K is regulated by IGF2BP3 in PDAC. (A) In GEPIA, IGF2BP3 was associated with UBE2K in PDAC. (B) Reverse transcription-quantitative PCR and (C) western blotting results indicated overexpression of IGF2BP3 led to upregulation of UBE2K in RNA and protein levels. (D) Reverse transcription-quantitative PCR and (E) western blotting results indicated knockdown of IGF2BP3 led to decrease of UBE2K in RNA and protein levels. (F) Shortened UBE2K RNA half-life by knockdown IGF2BP3 in BxPC-3 cells. *P<0.05, **P<0.01, ***P<0.001. UBE2K, ubiquitin-conjugating enzyme E2K; PDAC, pancreatic ductal adenocarcinoma; GEPIA, gene expression profiling interactive analysis; NC, negative control; si, short interfering.

the sphere was larger after UBE2K overexpression (Fig. 2F). Collectively, these data indicated that UBE2K overexpression promoted cell proliferation and stemness of PDAC *in vitro*.

UBE2K knockdown suppresses cell proliferation and stemness in PDAC. To further confirm the role of UBE2K in PDAC, UBE2K knockdown was induced in BxPC-3 and PANC-1cells using lentiviral vector. The RT-qPCR and western blotting results indicated that UBE2K was stably knocked down in PDAC cells (Fig. 3A and B). The knockdown of UBE2K restrained the proliferation of PDAC cells, as revealed in the CCK-8 and colony formation assays (Fig. 3C and D). In contrast to the results of UBE2K overexpression, the knockdown of UBE2K suppressed the protein expression of stemness-related genes, including NANOG and LIN28B in BxPC-3 and PANC-1 cells (Fig. 3E). Consistently, UBE2K inhibition also reduced the sphere formation ability (Fig. 3F), as the spheres reduced in size upon UBE2K knockdown. Collectively, these data suggested that the knockdown of UBE2K could reduce cell proliferation and stemness in PDAC.

UBE2K promotes PDAC growth in vivo. To investigate the oncogenic function of UBE2K in PDAC growth *in vivo*, a subcutaneous xenograft nude mouse model was established using BxPC-3 cells. The tumor was larger in the UBE2K overexpression group than in the control group (Fig. 4A). During the experiment, we measured the length and width every 5 days. The results revealed that the volume was larger in the UBE2K overexpression group (Fig. 4B). The tumor weight in the UBE2K overexpression group was also greater than that in the control group (Fig. 4C). Finally, the RNA and protein levels of UBE2K in the tumor tissues of nude mice were measured. The RNA and protein expression levels of UBE2K were higher in the UBE2K overexpression group (Fig. 4D and E).

To further verify the roles of UBE2K *in vivo*, shNC and shUBE2K cells were then injected into the nude mice. It was found that tumors from the shUBE2K groups were smaller than their control group counterparts (Fig. 4F). As expected, the volume and weight of tumors in the shUBE2K groups were also less than their control group counterparts (Fig. 4G and H). Additionally, the RNA and protein expression levels were also lower in the shUBE2K groups (Fig. 4I and J). To sum up, the results suggested that UBE2K is essential for PDAC tumor growth *in vivo*.

UBE2K is regulated by IGF2BP3 in PDAC. The above results indicated the prognostic and oncogenic roles of UBE2K in PDAC. However, the molecular regulation was unclear. As previously reported, IGF2BP3 is an RBP, which broadly participates in cancer progression by regulating its downstream targets. For example, IGF2BP3 stabilizes the long noncoding RNA CDKN2B-AS1 to promote proliferation, migration and invasion in renal clear cell carcinoma (25). IGF2BP3 cooperates with RMB15 to stabilize the expression of TMBOM6 in laryngeal cancer (26). IGF2BP3 has been shown to serve as a potential unfavorable factor for PDAC (27). As revealed by the analysis of the GEPIA database, IGF2BP3 expression was positively associated with UBE2K expression and statistically significant in PDAC (Fig. 5A). Thus, it was hypothesized that IGF2BP3 might regulate UBE2K expression in PDAC. To elucidate the regulation between IGF2BP3 and UBE2K, IGF2BP3 plasmids were transfected into BxPC-3 cells and the overexpression efficiency of IGF2BP3 measured by RT-qPCR and western blotting. As shown in Fig. 5B and C, the

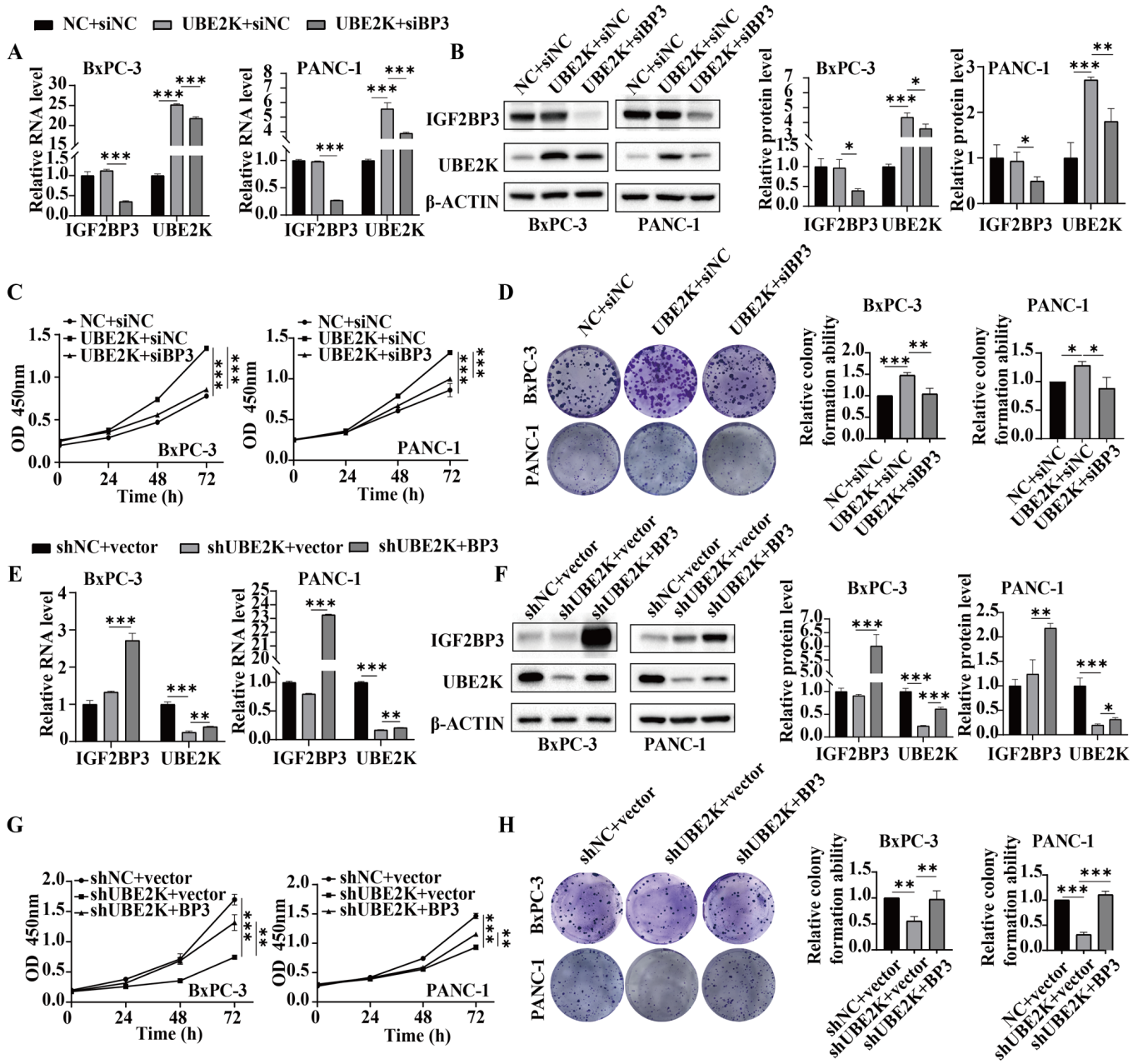

Figure 6. The effect of UBE2K can be revered by IGF2BP3 in PDAC. (A) Reverse transcription-quantitative PCR and (B) western blotting results in the groups of NC + siNC, UBE2K + siNC and UBE2K + siIGF2BP3. The (C) CCK-8 and (D) colony formation assays results in the groups of NC + siNC, UBE2K + siNC and UBE2K + siIGF2BP3. (E) Reverse transcription-quantitative PCR and (F) western blotting results in the groups of shNC + vector, shUBE2K + vector and shUBE2K + IGF2BP3. The (G) CCK-8 and (H) colony formation assays results in the groups of shNC + vector, shUBE2K + vector and shUBE2K + IGF2BP3. *P<0.05, **P<0.01, ***P<0.001. UBE2K, ubiquitin-conjugating enzyme E2K; PDAC, pancreatic ductal adenocarcinoma; NC, negative control; si, short interfering; sh, short hairpin.

overexpression of IGF2BP3 led to the upregulation of UBE2K at the RNA and protein levels. By contrast, the siRNA-mediated knockdown of IGF2BP3 decreased the RNA and protein expression of UBE2K (Fig. 5D and E). To determine if IGF2BP3 affects the RNA stability of UBE2K, IGF2BP3 siRNA was transfected in BxPC-3 cells and the cells treated with actinomycin D. The results demonstrated that IGF2BP3 knockdown notably decreased the RNA stability of UBE2K (Fig. 5F). Therefore, IGF2BP3 stabilized UBE2K to increase its expression.

IGF2BP3/UBE2K forms a functional axis in regulating the cell growth of PDAC. To explore whether IGF2BP3 contributes to the functional phenotype of the cell induced by UBE2K, IGF2BP3 was knockeddown by siRNA followed by overexpression of UBE2K. IGF2BP3 inhibition significantly decreased the cell proliferation induced by UBE2K overexpression, as revealed in the CCK-8 assay (Fig. 6A-C). Results of the colony formation assay (Fig. 6D) further confirmed that the knockdown of IGF2BP3 attenuated UBE2K induced growth in BxPC-3 and PANC-1 cells. In addition, IGF2BP3 was also re-expressed into the UBE2K knockdown cells (Fig. 6E and F). CCK-8 and colony formation assays showed that IGF2BP3 overexpression could successfully reverse the cell growth suppression caused by UBE2K knockdown

(Fig. 6G and H). In conclusion, IGF2BP3/UBE2K formed a functional axis in regulating cell growth in PDAC.

Discussion

PDAC is an extremely malignant tumor with a poor 5-year overall survival (2). It has a debilitating effect on the quality of life of afflicted individuals. Thus far, clear early-stage symptoms of PDAC have yet to be determined (28). Thus, it is critical to have thorough awareness of the molecular mechanisms underlying PDAC pathogenesis and then identify potential therapeutic targets for PDAC treatment.

Ubiquitin is highly conserved in eukaryotic cells and is a modified molecule composed of 76 amino acids through a cascade reaction of ubiquitin-activating enzyme (E1), ubiquitin-conjugating enzyme (E2) and ubiquitin-protein ligase (E3) that covalently binds and marks its target substrates (29). Subsequently, the ubiquitination-modified substrate protein is degraded by the 26S proteasome (29). UBE2K is a ubiquitin-coupled E2 enzyme. It serves essential roles in the progression of human neurodegenerative diseases (11-14). In PD, UBE2K is expressed at high levels in the patient's brain and is found to regulate the JNK signaling pathway in Aβ neurotoxicity (11). Meanwhile, the deficiency of UBE2K expression contributes to motor function impairment, which shows that UBE2K can serve as a promising biomarker for PD diagnosis (13). In types of human cancer, UBE2K is reported to be upregulated in gastric cancer (GC) and a high expression of UBE2K is associated with poor prognosis in patients with GC (16). It is also reported that UBE2K, acting as an oncogene, is downregulated by ixazomib and further demonstrated to be involved in ixazomib-induced cell apoptosis, cell cycle arrest, reactive oxygen species production and inhibition of myeloma cell proliferation (15).

The current study explored the function and molecular mechanism of UBE2K in the malignant progression of PDAC. First, it revealed that UBE2K was expressed at high levels in PDAC tissues and cells compared with normal tissues and normal human pancreatic ductal cells. High UBE2K expression predicted the poor prognosis of patients with PDAC. Second, the overexpression of UBE2K promoted the growth and stemness of PDAC cells, whereas the loss of UBE2K expression suppressed the growth and stemness of PDAC cells *in vitro*, which was also confirmed *in vivo* in subcutaneous xenograft mouse models. Third, the RNA-binding protein IGF2BP3 was found to be an upstream regulator of UBE2K that enhanced its expression by stabilizing UBE2K RNA. The overexpression or knockdown of IGF2BP3 led to the upregulation or downregulation of UBE2K at both RNA and protein levels. In addition, IGF2BP3 overexpression rescued cell growth inhibition caused by UBE2K knockdown in BxPC-3 and PANC-1 cells in CCK8 and colony plate experiments, whereas IGF2BP3 knockdown attenuated cell growth promotion induced by UBE2K overexpression. This indicated that IGF2BP3 and UBE2K may form the IGF2BP3/UBE2K axis in PDAC cells. Collectively, the findings illustrated the oncogenic role of UBE2K in PDAC *in vitro* and *in vivo* and clarified the IGF2BP3-mediated upregulation of UBE2K by enhancing the RNA stability of UBE2K. Further, the findings of the present study demonstrated that IGF2BP3 and UBE2K form a functional axis (IGF2BP3/UBE2K axis) that participates in the malignant progression of PDAC. This indicates the potential roles of the IGF2BP3/UBE2K axis in the prognosis of PDAC and as a therapeutic target in this disease.

However, the present study had some limitations. First, it did not analyze the association between UBE2K expression and tumor staging in patients with PDAC. Second, UBE2K is a ubiquitin ligase and its potential downstream targets regulated by ubiquitination need to be explored further.

In conclusion, the present study reported the function of the IGF2BP3/UBE2K axis in regulating PDAC cell growth and stemness for the first time to the best of the authors' knowledge. The findings elucidated a novel molecular mechanism underlying UBE2K function in PDAC progression. This can help improve the theoretical basis of PDAC carcinogenesis. In addition, the IGF2BP3/UBE2K axis might be a promising therapeutic target for PDAC.

Acknowledgments

Not applicable.

Funding

The present study was supported by the Research Foundation of Education of Zhejiang Province (grant no. Y202249315), National Natural Science Foundation of China (grant no. 82103295), Natural Science Foundation of Zhejiang Province (grant no. LQ22H160062), and Medical and Health Science Technology Project of Zhejiang Province (grant nos. 2019RC105 and 2022KY516).

Availability of data and materials

The datasets used and/or analyzed in the present study are available from the corresponding author on reasonable request.

Authors' contributions

XH and XT designed the study. WF conducted RT-qPCR, western blotting, CCK8, colony assay and wrote the original draft of the manuscript. XL, QL and JZ performed the experiments on nude mice. JG and JZ helped in the sphere formation assays. XH and XT confirm the authenticity of all the raw data and revised the manuscript. All authors read and approved the final manuscript.

Ethics approval and consent to participate

The animal experiments were approved (approval no. A20220046) by the Animal Ethics Committee of Zhejiang Provincial People's Hospital.

Patient consent for publication

Not applicable.

Completing interests

The authors declare that they have no competing interests.

References

1. Sung H, Ferlay J, Siegel RL, Laversanne M, Soerjomataram I, Jemal A and Bray F: Global Cancer Statistics 2020: GLOBOCAN estimates of incidence and mortality worldwide for 36 cancers in 185 countries. CA Cancer J Clin 71: 209-249, 2021.
2. Rahib L, Smith BD, Aizenberg R, Rosenzweig AB, Fleshman JM and Matrisian LM: Projecting cancer incidence and deaths to 2030: The unexpected burden of thyroid, liver, and pancreas cancers in the United States. Cancer Res 74: 2913-2921, 2014.
3. Nevala-Plagemann C, Hidalgo M and Garrido-Laguna I: From state-of-the-art treatments to novel therapies for advanced-stage pancreatic cancer. Nat Rev Clin Oncol 17: 108-123, 2020.
4. Grice GL and Nathan JA: The recognition of ubiquitinated proteins by the proteasome. Cell Mol Life Sci 73: 3497-3506, 2016.
5. Maxwell BA, Gwon Y, Mishra A, Peng J, Nakamura H, Zhang K, Kim HJ and Taylor JP: Ubiquitination is essential for recovery of cellular activities after heat shock. Science 372: eabc3593, 2021.
6. Salas-Lloret D and Gonzalez-Prieto R: Insights in post-translational modifications: Ubiquitin and SUMO. Int J Mol Sci 23: 3281, 2022.
7. Swatek KN and Komander D: Ubiquitin modifications. Cell Res 26: 399-422, 2016.
8. Middleton AJ, Teyra J, Zhu J, Sidhu SS and Day CL: Identification of ubiquitin variants that inhibit the E2 ubiquitin conjugating enzyme, Ube2k. ACS Chem Biol 16: 1745-1756, 2021.
9. Middleton AJ and Day CL: The molecular basis of lysine 48 ubiquitin chain synthesis by Ube2K. Sci Rep 5: 16793, 2015.
10. Cook BW, Lacoursiere RE and Shaw GS: Recruitment of ubiquitin within an E2 chain elongation complex. Biophys J 118: 1679-1689, 2020.
11. Song S, Kim SY, Hong YM, Jo DG, Lee JY, Shim SM, Chung CW, Seo SJ, Yoo YJ, Koh JY, *et al*: Essential role of E2-25K/Hip-2 in mediating amyloid-beta neurotoxicity. Mol Cell 12: 553-563, 2003.
12. de Pril R, Fischer DF, Roos RA and van Leeuwen FW: Ubiquitin-conjugating enzyme E2-25K increases aggregate formation and cell death in polyglutamine diseases. Mol Cell Neurosci 34: 10-19, 2007.
13. Su J, Huang P, Qin M, Lu Q, Sang X, Cai Y, Wang Y, Liu F, Wu R, Wang X, *et al*: Reduction of HIP2 expression causes motor function impairment and increased vulnerability to dopaminergic degeneration in Parkinson's disease models. Cell Death Dis 9: 1020, 2018.
14. Tak YJ and Kang S: The E2 ubiquitin-conjugating enzyme HIP2 is a crucial regulator of quality control against mutant SOD1 proteotoxicity. Biochim Biophys Acta Mol Basis Dis 1868: 166316, 2022.
15. Wang Q, Dong Z, Su J, Huang J, Xiao P, Tian L, Chen Y, Ma L and Chen X: Ixazomib inhibits myeloma cell proliferation by targeting UBE2K. Biochem Biophys Res Commun 549: 1-7, 2021.
16. Wu J, Tian B, Yang J, Huo H, Song Z, Yu J and Gu Y: Reduction of Hip2 suppresses gastric cancer cell proliferation, migration, invasion and tumorigenesis. Transl Cancer Res 9: 774-785, 2020.
17. Coppin L, Leclerc J, Vincent A, Porchet N and Pigny P: Messenger RNA life-cycle in cancer cells: Emerging role of conventional and non-conventional RNA-Binding proteins? Int J Mol Sci 19: 650, 2018.
18. Mancarella C and Scotlandi K: IGF2BP3 from physiology to cancer: Novel discoveries, unsolved issues, and future perspectives. Front Cell Dev Biol 7: 363, 2020.
19. Zhang N, Shen Y, Li H, Chen Y, Zhang P, Lou S and Deng J: The m6A reader IGF2BP3 promotes acute myeloid leukemia progression by enhancing RCC2 stability. Exp Mol Med 54: 194-205, 2022.
20. Wang C, Kong F, Ma J, Miao J, Su P, Yang H, Li Q and Ma X: IGF2BP3 enhances the mRNA stability of E2F3 by interacting with LINC00958 to promote endometrial carcinoma progression. Cell Death Discov 8: 279, 2022.
21. Wan W, Ao X, Chen Q, Yu Y, Ao L, Xing W, Guo W, Wu X, Pu C, Hu X, *et al*: METTL3/IGF2BP3 axis inhibits tumor immune surveillance by upregulating N (6)-methyladenosine modification of PD-L1 mRNA in breast cancer. Mol Cancer 21: 60, 2022.
22. Han J and Hu X: IGF2BP3stabilized SIX4 promotes the proliferation, migration, invasion and tube formation of ovarian cancer cells. Mol Med Rep 26: 232, 2022.
23. Tang Z, Li C, Kang B, Gao G, Li C and Zhang Z: GEPIA: A web server for cancer and normal gene expression profiling and interactive analyses. Nucleic Acids Res 45(W1): W98-W102, 2017.
24. Schmittgen TD and Livak KJ: Analyzing real-time PCR data by the comparative C(T) method. Nat Protoc 3: 1101-1108, 2008.
25. Xie X, Lin J, Fan X, Zhong Y, Chen Y, Liu K, Ren Y, Chen X, Lai D, Li X, *et al*: LncRNA CDKN2B-AS1 stabilized by IGF2BP3 drives the malignancy of renal clear cell carcinoma through epigenetically activating NUF2 transcription. Cell Death Dis 12: 201, 2021.
26. Wang X, Tian L, Li Y, Wang J, Yan B, Yang L, Li Q, Zhao R, Liu M, Wang P and Sun Y: RBM15 facilitates laryngeal squamous cell carcinoma progression by regulating TMBIM6 stability through IGF2BP3 dependent. J Exp Clin Cancer Res 40: 80, 2021.
27. Wang L, Zhang S, Li H, Xu Y, Wu Q, Shen J, Li T and Xu Y: Quantification of m6A RNA methylation modulators pattern was a potential biomarker for prognosis and associated with tumor immune microenvironment of pancreatic adenocarcinoma. BMC Cancer 21: 876, 2021.
28. Kamisawa T, Wood LD, Itoi T and Takaori K: Pancreatic cancer. Lancet 388: 73-85, 2016.
29. Hershko A: Ubiquitin: Roles in protein modification and breakdown. Cell 34: 11-12, 1983.